

A small-angle neutron scattering investigation of rigid polyelectrolytes under shear<sup>1</sup>E. Mendes,<sup>a\*</sup> S. Viale,<sup>a</sup> O. Santin,<sup>b‡</sup> M. Heinrich<sup>c</sup> and S. J. Picken<sup>a</sup><sup>a</sup>Polymer Materials Engineering, Delft University of Technology, Dutch Polymer Institute, Julianalaan 136, 2628 BL Delft, The Netherlands, <sup>b</sup>Universidade Estadual de Maringá, Maringá, Brazil, and <sup>c</sup>Institut für Festkörperforschung, Forschungszentrum, Jülich GmbH, D-52425 Jülich, Germany. Correspondence e-mail: e.mendes@tnw.tudelft.nl

Solutions of a rigid polyelectrolyte molecule, sulfo-poly(phenyleneterephthalamide) (SPTTA), in deuterated water have been investigated using small-angle neutron scattering. At low concentrations (1 wt%) the scattering spectrum presents a soft maximum similar to that of the interaction of rod-like objects. Two counterions are used, H<sup>+</sup> and Li<sup>+</sup>, and it is shown that aggregation is favoured as the proportion of Li<sup>+</sup> counterions increases. When kept at rest at room temperature, the solutions exhibit spontaneous birefringence. A 1 wt% solution was investigated under shear and it is shown that a very small shear rate is needed to produce a very strong alignment of rod-like objects. Such alignment saturates at high shear rates. Upon cessation of shear, a very long relaxation time is observed. The set of results strongly suggest aggregation of rigid polyelectrolyte molecules into long needles exhibiting very small cross sections.

© 2003 International Union of Crystallography  
Printed in Great Britain – all rights reserved

## 1. Introduction

Rigid-rod synthetic molecules are used in different industrial applications, some of the most common being fibre processing and fibre reinforcement (Kwolek, 1974). Such molecules are usually very difficult to solubilize, as in the case of poly(*p*-phenyleneterephthalamide) (PPTA), for which concentrated sulfuric acid is used during processing (Kwolek *et al.*, 1977). Industrial interest in modified water-soluble synthetic rigid-rod molecules lies, therefore, in their use in processing. A possible water-soluble modification of the PPTA molecule is the introduction of ionic groups in the backbone (Vandenberg *et al.*, 1989). Once in aqueous solution, such systems can also be potentially used as ion-conducting media and are candidates for batteries and fuel-cell membrane applications (Zhang *et al.*, 1999), while still being appropriate for classic industrial application.

The study of ionic synthetic rigid-rod molecules raises, however, more fundamental questions. For instance, liquid-crystalline phases have been reported (Picken *et al.*, 1990) for PPTA/sulfuric acid solutions, and one could conjecture that such phases could be spontaneously formed in their ionic counterparts in aqueous solutions, similar to those observed in aqueous solutions of natural rigid-rod molecules such as xanthan (Maret *et al.*, 1981; Rinaudo & Millas, 1982; Millas & Rinaudo, 1983) and DNA (Robinson, 1961) fragments.

The goal of the present study was to investigate solutions of a new water-soluble synthetic rigid-rod molecule, namely

sulfonated poly(*p*-phenyleneterephthalamide) (SPPTA). Different aspects of the solution properties of these new molecules will be addressed in the present paper. First, because of their potential use as ion-conducting media for batteries and fuel-cell applications, the structures of solutions containing different amounts of Li<sup>+</sup> counterions in the sulfonated backbone will be investigated. Second, because of the importance of processing ionic rigid-rod molecules, the behaviour of aqueous solutions under shear will be considered. Finally, the issue of spontaneous formation of a liquid-crystalline phase will be discussed.

## 2. Studied systems and methods

## 2.1. Synthesis

The monomer of sulfo-poly(phenyleneterephthalamide) (SPPTA), Fig. 1, has been synthesized as described by Vandenberg *et al.* (1989) and Viale *et al.* (2003).

**2.1.1. Materials.** Chlorotrimethylsilane (99.99%) (TMSCl) and *N,N*-dimethylacetamide (99.99%) (DMAc) (Aldrich Sure Seal) were used as received. Lithium chloride was dried under

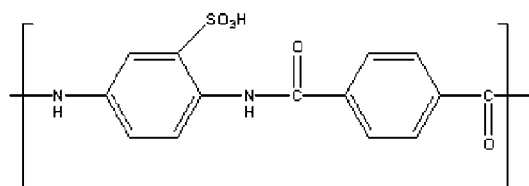


**Figure 1**  
The monomer of sulfo-poly(phenyleneterephthalamide) (SPPTA).

<sup>1</sup> This paper was presented at the XIIth International Conference on Small-Angle Scattering, Venice, Italy, 25–29 August 2002.

<sup>‡</sup> Present address: Lab. Dynamique des Fluides Complexes, CNRS/ULP UMR 7506, 4 rue Blaise Pascal, 67070 Strasbourg, France.

vacuum in an oven at 523 K overnight. Other solvents were technical grade. *p*-Phenylenediamine (sPPD; Fluka) and terephthalic acid chloride (TDC; Aldrich) were purified as described in the literature.

**2.1.2. Silylation.** The polycondensation and all transfer operations were carried out in flame-dried glassware and under argon because of the high moisture sensitivity of the silylated diamines and the polymerization reaction. The glassware was heated at 423 K and flushed with dry argon for 1 h. The reaction was carried out in an inert atmosphere. The reactor was charged with 10 g of sPPD (53 mmol), 200 ml of DMAc and 4.7 g of LiCl (0.11 mol). This solution was heated at 358 K until complete dissolution of LiCl and sPPD (the solution turned yellow). The solution was cooled with dry ice and acetone, the temperature dropping to 248 K. The mechanical stirrer was set at 1600 r.p.m. The dropping funnel was filled with 30 ml of TMSCl (0.237 mol). After addition, the ice bath was removed, allowing room temperature to be reached. Finally, the solution was heated at 313 K for 24 h, after which the reactor was left at room temperature. The solution was cooled with dry ice, the temperature dropping to 248 K.

**2.1.3. Polymerization.** The dropping funnel was filled with 10.8 g of TDC (53 mmol) dissolved in 60 ml of DMAc. The solution was added dropwise during 15 min. During this time, the temperature increased from 248 to 273 K. After addition, the ice bath was removed, allowing room temperature to be reached. The solution was then heated stepwise: 313 K for 1 h and 348 K for 1.5 h. At this time the solution was yellow and very viscous. This mixture was precipitated in 1200 ml of methanol. The suspension was filtered through a P2 frit. The fluffy yellow precipitate was dissolved in hot dimethylformamide (478 K). The solution was reprecipitated in 2 l of ether. The yellow powder was washed with 500 ml of methanol, 500 ml of acetone and 500 ml of ether. The goldish powder was dried in vacuum at 333 K overnight, leaving 19 g, yield 91%. The  $^1\text{H}$  and  $^{13}\text{C}$  nuclear magnetic resonance spectra of the SPPTA were consistent with the polymer structure. The

molecular weight was determined by viscosimetry and size-exclusion chromatography in concentrated sulfuric acid. The polymer (Schaeften, 1976) has a molecular weight of  $10000\text{ g mol}^{-1}$  and a polydispersity index of 1.4–1.8.

**2.1.4. Lithium content.** Different lithium counterion contents were obtained by adding powdered lithium oxide to the polymer samples. The solutions were prepared using distilled and demineralized water as a solvent. All these operations were carried out in a glove box because of the high reactivity of lithium oxide with air. These solutions were then boiled for 10 min and left in a ultrasonic bath for 2 h filled with hot water (343 K). After the procedure, a clear yellow solution was obtained.

## 2.2. Sample preparation and conditioning

The polymer powders were dissolved in  $\text{D}_2\text{O}$  (1 wt%). The solutions were heated at 373 K for 5 min in sealed tubes and then subjected to ultrasound mixing for at least 2 h at 333 K. Conditioning at 333 K prevents rapid appearance of birefringence. Such birefringence is observed for samples that rest at 293 K after preparation. At those temperatures, when kept at rest in test tubes, birefringence develops in the sample, starting in the upper part of the tube. The developing time depends on the polymer concentration and lithium counterion content. For isotropic samples, of 1 wt% polymer and containing a mass fraction of lithium of 0.28 wt% (2 wt% corresponds to full lithium counterion content), birefringence starts to develop immediately at 293 K and seems to stabilize after a few hours. A photograph of such a sample, one month old, is presented as Fig. 2. Under the optical microscope no macroscopic structures can be observed.

Prior to the shear experiments, the polymer solutions were re-heated to 373 K for 2 min before they were poured into a Couette cell, which was previously set to 348 K. The Couette had a 2 mm gap and the temperature was controlled with a thermal bath, ranging from 298 to 348 K during this set of experiments. Shear experiments were carried out at 298 K. Before application of shear, the sample rested in the Couette for at least 2 h at 298 K.

## 2.3. Small-angle scattering experiments

Isotropic experiments were performed at the KWS2 spectrometer at the Institut für Festkörperforschung, Forschungszentrum, Jülich, Germany. An incident neutron wavelength of  $7\text{ Å}$  was employed, with sample–detector distances of 2 m and 8 m, with collimations of 4 m and 8 m, respectively. Standard procedures of data treatment were applied to the raw data, including division by the flat incoherent scattering of water and subtraction of background incoherent scattering.

Shear experiments were carried out at the PAXY spectrometer at Laboratoire Leon Brillouin, CEA-CNRS, Saclay (France), with a  $128 \times 128$  two-dimensional detector with  $0.25\text{ cm}^2$  cells. A sample–detector distance of 2.5 m and an incident neutron wavelength of  $8\text{ Å}$  were employed. Standard procedures of data treatment were applied to the raw data.

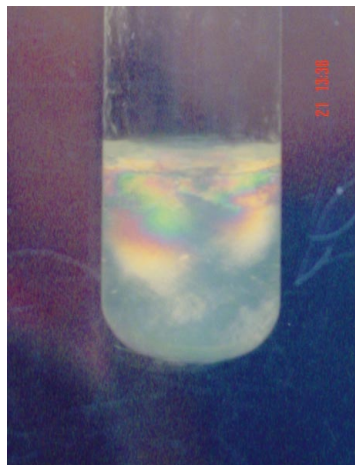


**Figure 2**  
Cross-polarized photograph of a 1 wt% solution of SPPTA in heavy water after thermal treatment and after one month at rest at 293 K.

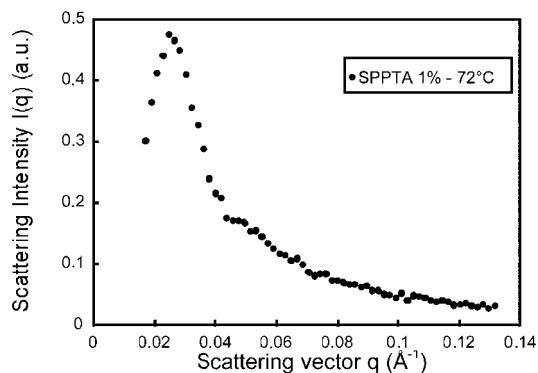


**Figure 3**

Scattering intensity as a function of scattering vector for a 1 wt% solution of the SPPTA polymer described in §2.1 in heavy water at 345 K. The lithium counterion content is 0.28 wt%.

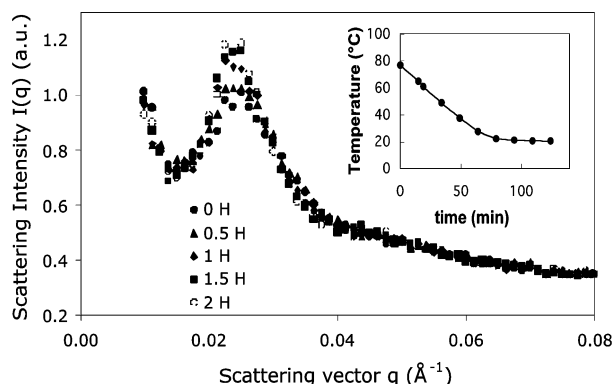


**Figure 4**

Scattering intensity as a function of scattering vector,  $q$ , for a 1 wt% solution of SPPTA during the cooling process from 345 to 293 K. The inset shows the Couette cell temperature with time.

Three different shear rates were applied to the samples: 12.5, 125 and 2500  $\text{s}^{-1}$ . Data were also partitioned according to the parallel and perpendicular directions to the applied shear, using angular sectors of 15°.

### 3. Results

#### 3.1. Solutions at rest

At rest, a 1 wt% solution of SPPTA presents a scattering maximum at small angles. A typical spectrum of scattering intensity *versus* the modulus  $q$  of the scattering vector is given in Fig. 3 for a temperature of 345 K ( $q = 4\sin\theta/\lambda$ , where  $\theta$  is half the scattering angle and  $\lambda$  is the neutron wavelength).

As the temperature is decreased, the scattering maximum sharpens, revealing an increase of ordering at a mesoscopic level. This effect is displayed in Fig. 4. Although the temperature of the Couette cell stabilizes in about 1 h (see inset of Fig. 4), the scattering maximum needs more time (about 2 h) to exhibit stabilization. In Fig. 4, each spectrum corresponds to the scattered intensity cumulated over 1 h. An important point, however, is that no strong variation of the intensity at high angles is observed during the cooling process,

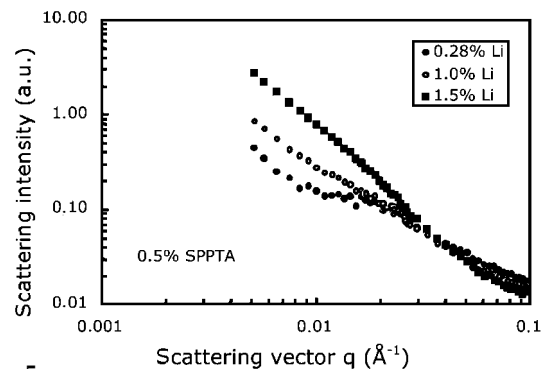


**Figure 5**

Scattering intensity as a function of scattering vector for a 0.5 wt% solution of SPPTA in heavy water at 293 K. Different  $\text{Li}^+$  contents are displayed. A concentration of 2 wt% Li corresponds to full  $\text{Li}^+$  counterion content.

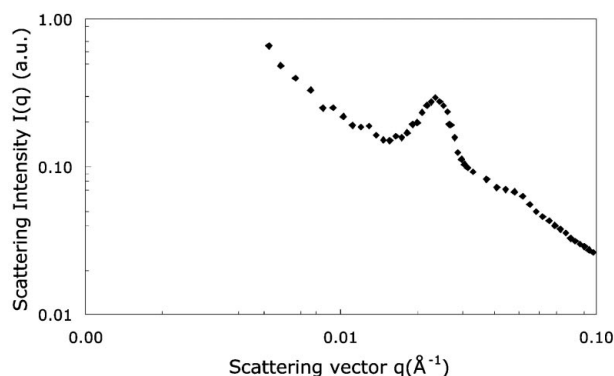


**Figure 6**

Scattering intensity as a function of scattering vector for the birefringent upper part taken separately from the tube. The scattering is not very different from that of Fig. 4.

revealing basically no change in the average polymer concentration.

The position and intensity of the scattering maximum depends on polymer concentration (Wang *et al.*, 2001), but, at the same time, the structure of the solution is strongly dependent on the amount of  $\text{Li}^+$  counterions. The effect of increase in the  $\text{Li}^+$  content on the structure of the solutions can be seen in Fig. 5. Basically, the increase in the  $\text{Li}^+$  content favours the formation of aggregates, as can be seen in Fig. 5: the small upturn present at small angles strongly increases with increasing amount of  $\text{Li}^+$  counterions. If the amount of added lithium is high enough, precipitation is observed with kinetics that seem to be much faster than indicated in §2.2.

As reported above, spontaneous birefringence is observed in the upper part of the test tube for SPPTA solutions in deuterated water when cooled to room temperature. The scattering of this birefringent upper part is displayed in Fig. 6. The curve exhibits a scattering maximum similar to that of the original solution, at the same position but slightly sharper. It is plotted on a log-log scale in order to enhance the second-order maximum. The average shear viscosity of the solution at 293 K is not very high: 0.05 Pa s for a shear rate of 12.5  $\text{s}^{-1}$ , decreasing to 0.016 Pa s for 251  $\text{s}^{-1}$  for samples prepared and measured under the same conditions of the neutron scattering

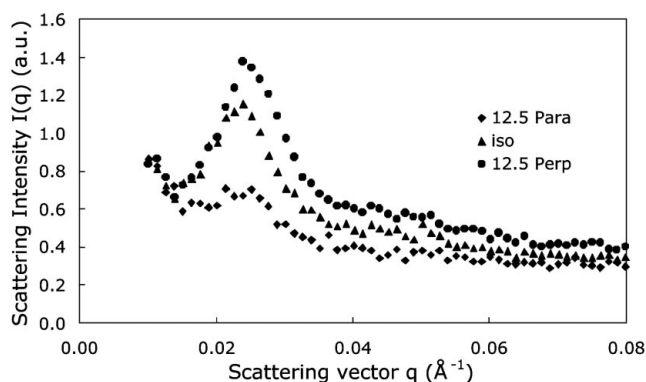


**Figure 7**  
Scattered intensity under shear as a function of  $q$  for a 1 wt% solution of SPPTA at 293 K, 0.28 wt%  $\text{Li}^+$ , displayed together with the isotropic state. The applied shear rate is  $\dot{\gamma} = 12.5 \text{ s}^{-1}$ .

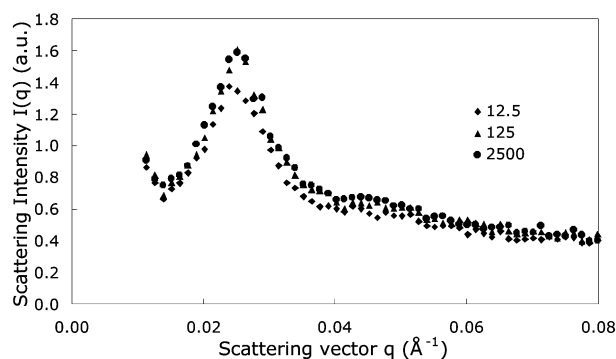


**Figure 8**  
Scattered intensity in the perpendicular direction as a function of  $q$  for the solution of Fig. 7 at different shear rates ( $\text{s}^{-1}$ ).

shear experiments. The upper part of the solution seems to be more viscous than the lower part, but it was not measured separately. One possible explanation for the ensemble of results may be the spontaneous formation of needle-like aggregates (Chu *et al.*, 1995). Despite the observation of spontaneous birefringence in the upper part of the tube, the nature of the solution seems to be the same throughout the test tube.

### 3.2. Solutions under shear

The scattering maximum at small angles mentioned above corresponds to a ring of stronger intensity in the centre of the observable window when a two-dimensional detector is used in the scattering experiment. Under the action of shear, the scattering ring at small angles transforms into two spots in the direction perpendicular to the applied shear, while it is, therefore, dramatically suppressed in the direction parallel to the shear. This scattering increase in the perpendicular direction is associated with rod-like objects that align in the direction of flow. It should be stressed that this happens even for very small shear rates, since in order to align isolated polyelectrolyte molecules, far stronger shear rates than those used here are needed (Millas *et al.*, 1996).

Although a strong alignment is observed under shear, it seems that no restructuring of the solution occurs during the application of shear, such as the shear-induced aggregation

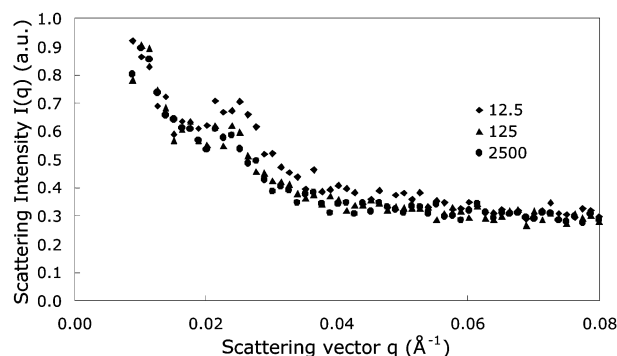


**Figure 9**  
Same as Fig. 8 for the intensity scattered in the parallel direction.

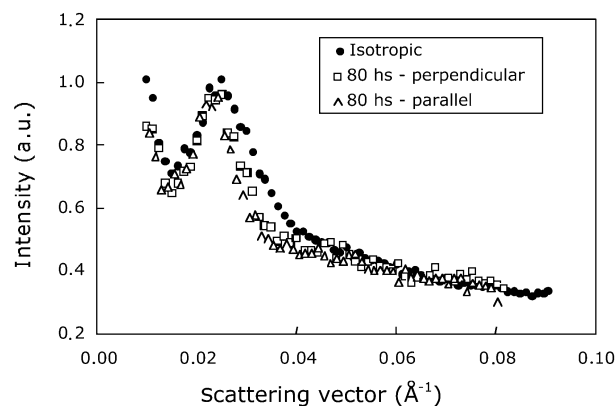


**Figure 10**  
Scattered intensity in the parallel and perpendicular directions 80 h after cessation of shear. The isotropic spectrum before shearing is also shown.

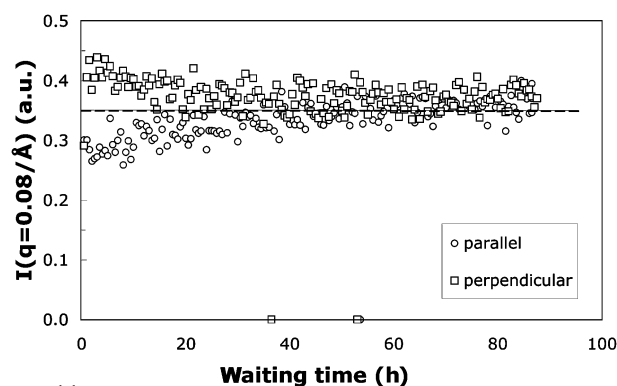


**Figure 11**  
Scattered intensity in the parallel and perpendicular directions at  $q = 0.08 \text{ Å}^{-1}$  as a function of time after cessation of flow. Data relates to the 1 wt% SPPTA solution of Figs. 8 and 9. The dashed line corresponds to the initial value before application of shear.

observed in ionic worm-like surfactant micelles under shear (Oda *et al.*, 2000). In the present case, contrary to the worm-like micelle case, the position of the maximum of intensity does not change with shear rate. This is illustrated in Fig. 7, where the scattering intensity in the parallel and perpendicular directions as a function of the scattering vector is plotted. The isotropic scattering before application of shear is also displayed.

The effect of different shear rates on alignment is displayed in Figs. 8 and 9 where the scattering intensities in the perpendicular and parallel directions are plotted for different

shear rates. As the shear rate is increased, an increase of intensity in the perpendicular direction and the suppression of intensity in the direction parallel to the shear is observed. As can be seen from the data, very small shear rates are enough to induce a strong alignment, namely,  $\gamma = 12.5 \text{ s}^{-1}$  in the present case. Such an increase in alignment seems to level off after a given shear rate value, as can be clearly seen by comparison of the last two shear rates (125 and  $2500 \text{ s}^{-1}$ ). After cessation of flow, the system was allowed to relax at rest while a spectrum was recorded every 30 min. In Fig. 10, the intensities in the parallel and perpendicular directions are plotted after a very long waiting time (80 h) together with the isotropic spectrum before application of shear. It can be seen from Fig. 10 that after such a long waiting time, the scattering at high  $q$  values practically superimposes to the original isotropic spectrum. This suggests that no strong variation of the polymer concentration due to ageing or to phase separation occurs, since at these scales the scattering intensity is proportional to the polymer volume fraction. A marked difference with respect to the initial isotropic spectrum is, however, observed at the scattering maximum: it is sharper than the original one while the position remains the same. This can be attributed to the increase of translational order in the sample with time. The detailed variation of the maximum width with time is under study and will be considered in a further publication.

Despite the small maximum sharpening reported above, it is possible to obtain a qualitative alignment relaxation time from data if one focuses on high scattering vector values. Such relaxation time is related to rotational diffusion of the rod-like objects in solution and it can be roughly estimated if one plots the intensity at high angles as a function of time. In Fig. 11, the scattering intensity for a fixed scattering vector,  $q = 0.08 \text{ \AA}^{-1}$ , is plotted against time after cessation of flow, for the parallel and perpendicular directions. It is clearly seen from the figure that even after 87 h, the variation of intensity at high  $q$  values is less than 5% of the original value before application of shear, attesting to the very small variation in polymer concentration. Despite the noise in data, one can estimate a relaxation time of the order of 30 h.

The set of results presented above, namely, (i) spontaneous birefringence, (ii) a scattering maximum at small angles for very low polymer concentrations, (iii) an extremely strong alignment response of the system to rather small applied shear rates, and (iv) a very long relaxation time after cessation of shear, suggest that the system is composed of rod-like objects that are far longer than the original polyelectrolyte molecules ( $\sim 500 \text{ \AA}$ ). The set of results can be explained if needle-like objects are formed after thermal treatment of the solution. Longer than the original polyelectrolyte molecules, they would respond much more readily to the application of shear. The formation of aggregates of rigid-rod polyelectrolytes has been reported before (Chu *et al.*, 1995). In the present case, such objects are not visible under the optical microscope. If needles are present in the studied solutions, they should exhibit very small sub-optical cross sections, perhaps of nanometre size. The question of the cross-section size of aggregating rigid polyelectrolytes has been addressed recently

from a theoretical point of view (Ha & Liu, 1997) and detailed investigations of our samples are in progress.

The appearance of the birefringence in the upper part of the tube, which is time and temperature dependent, attests to the ageing of the solution, although one cannot, without ambiguity, associate this spontaneous birefringence with a true liquid-crystal phase. It is possible that larger needles experiencing larger 'precipitation' forces would tend to migrate to the lower part of the solution faster than smaller ones. Since rotation of needles is very slow, as shown by relaxation-time estimations, migration favours needles with long axes in the vertical direction. As a result of a selective migration mechanism, horizontally aligned needles are expected to be preferentially located at the upper part of the tube, giving rise to a strong birefringence in that region of the sample. This hypothesis needs, however, to be investigated further.

#### 4. Conclusions

We have reported in this paper a small-angle neutron scattering study on rod-like polyelectrolytes in heavy water, namely, sulfo-poly(*p*-phenyleneterephthalamide) (SPPTA). At rest, the scattering curves exhibit a scattering maximum at a finite scattering value and a small upturn at small angles. The scattering maximum is related to the scattering of rod-like objects, not necessarily single molecules, while the upturn is attributed to aggregates that are probably present at larger scales. The counterions present in the sample are either  $\text{H}^+$  or  $\text{Li}^+$  and it is shown that as the proportion of  $\text{Li}^+$  counterions is increased, the solution exhibits a stronger tendency to aggregate. At the same time, the upturn present at small angles strongly increases with increasing amount of  $\text{Li}^+$  counterions. Similar behaviour is observed even for small amounts of  $\text{Li}^+$ .

When left at rest at room temperature, the upper parts of the solutions exhibit strong birefringence. Studied separately, they also exhibit a scattering maximum similar to that observed for the lower part of the solutions, with the same  $q$  position as that of the lower part. Both parts seem very similar in nature and it was suggested that the upper part is richer in larger needle-like aggregates that are preferentially aligned horizontally. A mechanism for selective diffusion of larger needles towards the lower part is proposed.

The effect of shear on the solutions was also investigated. It was shown that a strong alignment of rod-like objects, which are larger than the original molecules, is obtained even for a very low shear rate ( $12.5 \text{ s}^{-1}$ ). Alignment increases with shear rate and it seems to saturate at high shear values. After cessation of flow, the system was allowed to relax and data suggest that the isotropic state is recovered only after  $\sim 30 \text{ h}$ . It was also shown that the scattering maximum after long waiting time becomes sharper. At present, this is attributed to an increase in translational order. Detailed measurements of

alignment and relaxation after cessation of flow are under study and will be presented in a forthcoming publication.

The authors thank Dr L. Noirez (LLB CNRS, Saclay) for her help with the neutron scattering experiments and the Couette setup. OS and EM kindly acknowledge a Franco-Brazilian CAPES/COFECUB bilateral research program. EM would also like to thank J. Groenewold for helpful discussions. The authors are grateful for the constructive comments of both referees. This work forms part of the research program of the Dutch Polymer Institute (DPI).

## References

- Chu, G. Y., Evan, Y., Xu, Z. S., Lee, C. M., Sek, C. K. F., Okamoto, Y., Pearce, E. M. & Kwei, T. K. (1995). *J. Polym. Sci. B*, **33**, 71–75.
- Ha, B.-Y. & Liu, A. J. (1997). *Phys. Rev. Lett.* **79**, 1289–1292.
- Kwolek, S. L. (1974). US patent 3819587.
- Kwolek, S. L., Morgan, P. W., Schaeffgen, J. R. & Gulrich, L. W. (1977). *Macromolecules*, **10**, 1390–1396.
- Maret, G., Millas, M. & Rinaudo, M. (1981). *Polym. Bull.* **4**, 291–297.
- Millas, M., Lindner, P., Rinaudo, M. & Borsali, R. (1996). *Macromolecules*, **29**, 473–474.
- Millas, M. & Rinaudo, M. (1983). *Polym. Bull.* **10**, 271–273.
- Oda, R., Weber, V., Lindner, P., Pine, D. J., Mendes, E. & Schosseler, F. (2000). *Langmuir*, **16**, 4859–4863.
- Picken, S. J., Aerts, J., Visser, R. & Northolt, M. G. (1990). *Macromolecules*, **23**, 3849–3854.
- Rinaudo, M. & Millas, M. (1982). *Carbohydr. Polym.* **2**, 264–269.
- Robinson, C. (1961). *Tetrahedron*, **13**, 219–226.
- Schaeffgen, R. (1976). *Polym. Prep.* **17**, 69–74.
- Vandenberg, E. J., Diveley, W. R., Filar, L. J., Patel, S. R. & Barth, H. G. (1989). *J. Polym. Sci. Part A Polym. Chem.* **27**, 3745–3757.
- Viale, S., Jager, W. F. & Picken, S. J. (2003). Submitted.
- Wang, D., Jyotsana, L., Moses, D., Bazan, G. C. & Heeger, A. J. (2001). *Chem. Phys. Lett.* **348**, 411–415.
- Zhang, Y., Litt, M., Savinell, R. & Wainwright, J. (1999). *Polym. Preprints*, **40**, 480–481.